Original Article
Developing new ceramide analogs against non-small cell lung cancer (NSCLC)

Lu Dai[1], Navneet Goyal[2], Jiawang Liu[3], Maryam Foroozesh[2], Zhiqiang Qin[1]

[1]Department of Pathology, Winthrop P. Rockefeller Cancer Institute, University of Arkansas for Medical Sciences, 4301 W. Markham St., Little Rock, AR 72205, USA; [2]Department of Chemistry, Xavier University of Louisiana, 1 Drexel Drive, New Orleans, LA 70125, USA; [3]Department of Pharmaceutical Sciences, College of Pharmacy, University of Tennessee Health Science Center, Memphis, TN 38163, USA

Abstract: Non-small cell lung cancer (NSCLC) constitutes the predominant form of lung cancer and stands as the leading cause of cancer-related mortality in the United States. Conventional chemotherapy and radiotherapy yield suboptimal responses in a significant portion of lung cancer patients, resulting in a discouraging 5-year survival rate of approximately 15%. Despite advancements in targeted therapy and immunotherapy, many NSCLC patients exhibit either negligible or partial responses, emphasizing the pressing necessity for the discovery of innovative anti-cancer agents. Our previous study demonstrated that ABC294640, an inhibitor of one of the key enzymes in sphingolipid metabolism, sphingosine kinase 2 (SphK2), displayed anti-NSCLC activities *in vitro* and *in vivo*. In the current study, through the screening of a series of newly synthesized ceramide analogs, we have identified new compounds, particularly analogs 403 and 953, that exhibit potent anti-NSCLC activities. These compounds induce significant NSCLC apoptosis by elevating intracellular pre-apoptotic ceramide and dihydro(dh)-ceramide production. Lipidomics analyses further elucidate the alterations in ceramide and dh-ceramide species signature/proportion across different NSCLC cell-lines induced by these novel ceramide analogs. Treatments with ceramide analogs 403 and 953 remarkably inhibit NSCLC progression *in vivo* without observable toxicity. Collectively, these findings establish a foundation for the development of promising sphingolipid-based therapies aimed at enhancing the prognosis of NSCLC.

Keywords: NSCLC, lung cancer, ceramide, ceramide analogs, sphingolipid

Introduction

Lung cancer stands as the leading cause of cancer-related fatalities in the United States, projecting an estimated 127,070 deaths in 2023, with 67,160 in men and 59,910 in women [1]. Additionally, it ranks as the second most diagnosed cancer in the U.S., anticipating approximately 234,340 new cases in 2023 [1]. The disease encompasses two primary classifications based on treatment response and prognosis: small cell lung cancer (SCLC) and non-small cell lung cancer (NSCLC), the latter representing 85-90% of cases [2]. Clinically, a significant proportion of lung cancer patients exhibit poor responses to conventional chemo-/radio-therapeutic approaches, resulting in a grim 5-year survival rate of around 15% [3]. While the recent advent of targeted therapy and immunotherapy has offered renewed hope to NSCLC patients, the outcomes remain unsatisfactory. Targeted therapeutic drugs, such as Gefitinib, initially exhibit positive effects by inhibiting mutated epidermal growth factor receptor (EGFR). However, drug resistance inevitably develops after 10 months of treatment, leading to fatal outcomes [4]. Similarly, immune checkpoint inhibitors such targeting PD-1 and PD-L1 have demonstrated clinical success, improving overall survival in certain NSCLC patients. Yet, only 15-20% of patients respond to this therapy, and its affordability poses a substantial challenge, with a single course of treatment exceeding $100,000 [5, 6]. Moreover, reports of resistance to immunotherapy and hyper-progressive disease during checkpoint inhibitors treatment underscore the need for a deeper understanding of lung carcinogenesis mechanisms and the development of novel therapeutic agents [7, 8].

Sphingolipid biosynthesis involves the conversion of ceramides into sphingosine, which is subsequently phosphorylated by sphingosine kinase isoforms (SphK1 or SphK2) to generate sphingosine-1-phosphate (S1P) [9, 10]. Bioactive sphingolipids, including ceramides and S1P, act as signaling molecules regulating apoptosis and tumor cell survival. ABC294640, a highly selective small molecule inhibitor of SphK, has demonstrated significant anti-tumor effects across various cancers [13-16]. Previous studies, including a Phase I clinical trial, have indicated promising results for ABC294640 in patients with advanced solid tumors [17]. Our prior research demonstrated the anti-NSCLC activities of ABC294640 *in vitro* and *in vivo*, through inducing intracellular ceramide and dihydro(dh)-ceramide species within cancer cells [18].

To advance sphingolipid metabolism-targeted therapies, we synthesized new ceramide analogs with sulfonamide, amide, and/or specific aromatic modifications in the ceramide side chain or backbone. These modifications aimed to enhance anti-proliferation activity, regulate ceramide metabolism, and improve analog stability. Our current study screens a range of new ceramide analogs, identifying analogs 403 and 953 as effective anti-NSCLC agents *in vitro* and *in vivo*, inducing tumor cell apoptosis. Lipidomics analyses provide detailed insights into how treatment with these new ceramide analogs alters the ceramide signature, including the increase of different ceramide and dh-ceramide species, and changes in their proportion within NSCLC cells.

Materials and methods

Cell culture and reagents

NSCLC cell-lines (A549, H460, H1299) were generously provided by Dr. Hua Lu at Tulane University and cultured in RPMI-1640 medium supplemented with 10% fetal bovine serum and 1% penicillin & streptomycin. Experiments utilized cells harvested at low (<20) passages. The synthesis of new ceramide analogs was conducted by Dr. Maryam Foroozesh's group at Xavier University of Louisiana.

Syntheses of the new ceramide analogs 403 and 953

Synthesis of analog 403: As previously reported, for the synthesis of analog 403, D-sphingosine was reacted with phenylacetyl chloride (1 eq.) in the presence of sodium bicarbonate as a base and dichloromethane (DCM) as solvent [19].

Synthesis of analog 953: Boc-serine (1 eq.) was coupled with tetradecyl amine (1.1 eq.) to get the intermediate. N,N'-dicyclohexylcarbodiimide (DCC, 1.1 eq.) was used as a coupling reagent. 4-Methyl-morpholine (3.0 eq.) was used as a base, and dichloromethane was the solvent. The boc-(*tert*-butyl ether) group was then cleaved using trifluoroacetic acid (TFA, 2.5 eq.) in DCM to give the free amine, which was further reacted with 4-methylphenyl sulfonyl chloride (1.1 eq.) in the presence of a mild base, triethyl amine (3.0 eq.), in DCM. The final product, analog 953, was purified using combi-flash flash chromatography (hexane: ethyl acetate as the solvent system). GC-MS showed >99% purity. m/z: 456, 455, 454. ^{1}HNMR (CDCl$_3$, 300 MHz) δ = 7.76 (d, J = 8.4 Hz, 2H), 7.29 (d, J = 8.4 Hz, 2H), 6.89 (t, J = 5.5 Hz, 1H), 3.93-3.87 (m, 1H), 3.75 (t, J = 4.1 Hz, 1H), 3.45-3.38 (m, 2H), 3.23-3.06 (m, 2H), 2.42 (s, 3H), 1.41 (t, J = 5.5 Hz, 2H), 1.32-1.20 (m, 23H), 0.89 (t, J = 6.6 Hz, 3H). ^{13}C NMR (CDCl$_3$, 75 MHz) δ = 14.1, 21.5, 22.6, 26.8, 29.2, 29.3, 29.4, 29.5, 29.6, 29.6, 29.6, 29.7, 31.9, 39.9, 57.8, 62.4, 127.2, 129.9, 136.3, 144.0, 169.5.

Cell proliferation and apoptosis assays

Cell proliferation was assessed using the WST-1 Assay (Roche, Indianapolis, Indiana, USA). After treatment, 10 µL/well of WST-1 reagent was added to 96-well plates and incubated for 3 h at 37°C in 5% CO$_2$. Absorbance at 490 nm was measured using a microplate reader. Flow cytometry with the FITC-Annexin V/propidium iodide (PI) Apoptosis Detection Kit I (BD Pharmingen, San Jose, California, USA) was employed for quantitative apoptosis assessment, analyzed on a FACS Calibur 4-color flow cytometer (BD Bioscience, San Jose, California, USA).

Sphingolipid analyses

Quantification of sphingolipid species was performed using a Thermo Finnigan TSQ 7000 triple-stage quadruple mass spectrometer operating in Multiple Reaction Monitoring (MRM) positive ionization mode (Thermo Fisher Scientific, Waltham, Massachusetts, USA). Quantification was based on calibration curves generated by spiking an artificial matrix with known amounts of target standards and an equal amount of the internal standard. The tar-

get analyte:internal standard peak area ratios from each sample were compared with the calibration curves using linear regression. Final results were expressed as the ratio of sphingolipid normalized to total phospholipid phosphate level using the Bligh and Dyer lipid extract method [20].

Nude mice xenograft models

Cells were counted and washed once in ice-cold PBS. 5×10^5 H460 cells in 50 µL PBS plus 50 µL growth factor-depleted Matrigel (BD Biosciences, San Jose, California, USA) were injected subcutaneously into the flank of nude mice (Jackson Laboratory, Sacramento, California, USA). Five days after this injection, the mice were randomly separated into three groups and received i.p. injection with vehicle, ceramide analog 403 or 953 (25 mg/kg of body weight dissolved in PEG:ddH$_2$O as 1:1), 3 days/week. The mice were observed and measured every 2-3 days for the presence of palpable tumors. After the mice were sacrificed, the tumors were excised for subsequent analyses. All protocols were approved by the University of Arkansas for Medical Sciences Animal Care and Use Committee in accordance with national guidelines.

Immunoblotting

Total cell lysates (20 µg) were resolved by 10% SDS-PAGE, transferred to nitrocellulose membranes, and immunoblotted with antibodies to cleaved caspase 3 and 9 (Cell Signaling). GAPDH served as the loading control (Cell Signaling). Immunoreactive bands were identified using an enhanced chemiluminescence reaction (Perkin-Elmer) and visualized by autoradiography.

Statistical analysis

Significance for differences between experimental and control groups were determined using the two-tailed Student's *t*-test. The 50% Inhibitory Concentrations (IC$_{50}$) were calculated by using GraphPad Prism 9.

Results

Identification of new ceramide analogs with effective anti-NSCLC activities

Using the WST-1 Cell Proliferation Assay, we initially screened a series of new ceramide ana-logs (a total of 7 new compounds for which the structures and molecular weight are shown in **Figure 1A**). Most of these ceramide analogs displayed effective inhibition of the growth across the three NSCLC cell-lines (A549, H460, and H1299) tested (**Figure 1B**). Two ceramide analogs, *N*-((2S,3R,E)-1,3-dihydroxyoctadec-4-en-2-yl)-2-phenylacetamide (analog 403) and (S)-3-hydroxy-2-((4-methylphenyl)sulfonamide)-*N*-tetradecylpropanamide (analog 953), were selected for subsequent experiments due to their high efficacy. Their synthetic pathways are shown in **Figure 2A**, **2B**, and described in the Methods. Using a range of doses, we found that both analogs 403 and 953 showed a dose-dependent inhibition of growth of the three NSCLC cell-lines (**Figure 3A-C**). The 50% Inhibitory Concentrations (IC$_{50}$) of analog 403 was at ~2-10 µM, and the IC$_{50}$ of analog 953 was at ~12-18 µM, which were comparable to those of ABC294640 on NSCLC cell-lines (~7-9 µM) reported [18].

Treatment with the two new ceramide analogs induces apoptosis in NSCLC cells

We next sought to determine the underlying mechanisms for anti-NSCLC activities of the new ceramide analogs. Using flow cytometry, we found that both analogs 403 and 953 induced significant apoptosis in NSCLC cells (**Figure 4A**, **4B**). In detail, we found that treatment with these ceramide analogs increased subpopulation of both early (Annexin V+/PI-, ~8-15 folds) and late (Annexin V+/PI+, ~5-25 folds) apoptotic cells, when compared to the vehicle control. We also analyzed cell cycle in the same treatment conditions, and found that these ceramide analogs only slightly affected the NSCLC cell cycle (data not shown).

Treatment with the two new ceramide analogs increases the production of intracellular ceramides and dh-ceramides and alters their proportion in NSCLC cells

Mass spectrometric-based lipidomics analyses were used to quantify intracellular levels of bioactive ceramide/dh-ceramide species in NSCLC cell-lines. We found that both analogs 403 and 953 increased the production of most of the individual ceramide and dh-ceramide species, including C14~C26-Cer and dhC14~dhC26-Cer in the NSCLC cell-lines, A549 and H460, respectively (**Figures 5** and **6**). However, we observed different changes for some indi-
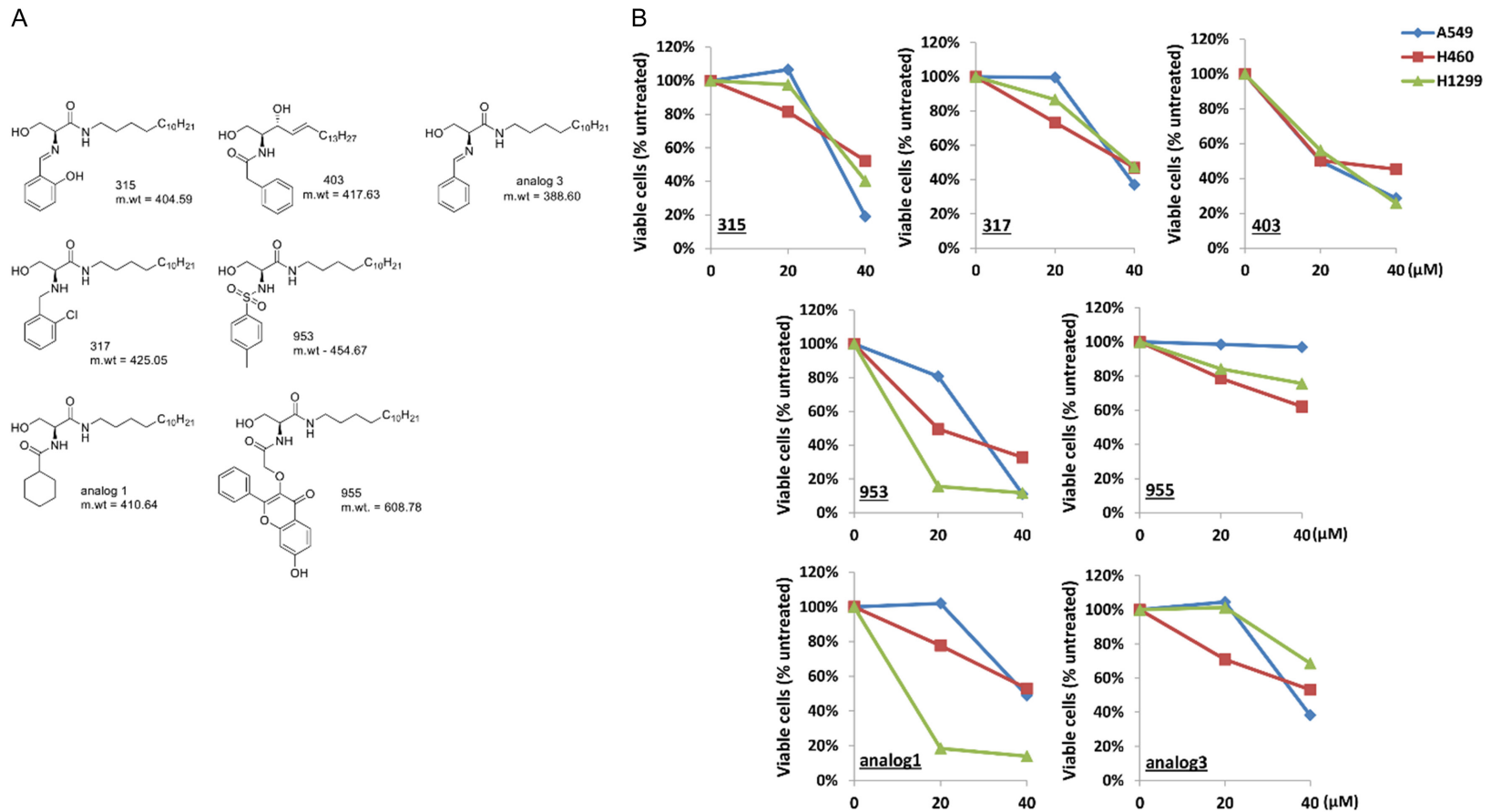
Figure 1. The screening of new ceramide analogs with anti-NSCLC activities. A. The chemical structures of our new synthetic ceramide analogs with molecular weight. B. NSCLC cell-lines A549, H460, and H1299 were incubated with the indicated concentrations of ceramide analogs for 72 h; cell proliferation was measured using the WST-1 assays. The experiments were repeated twice and one representative experimental results were shown.
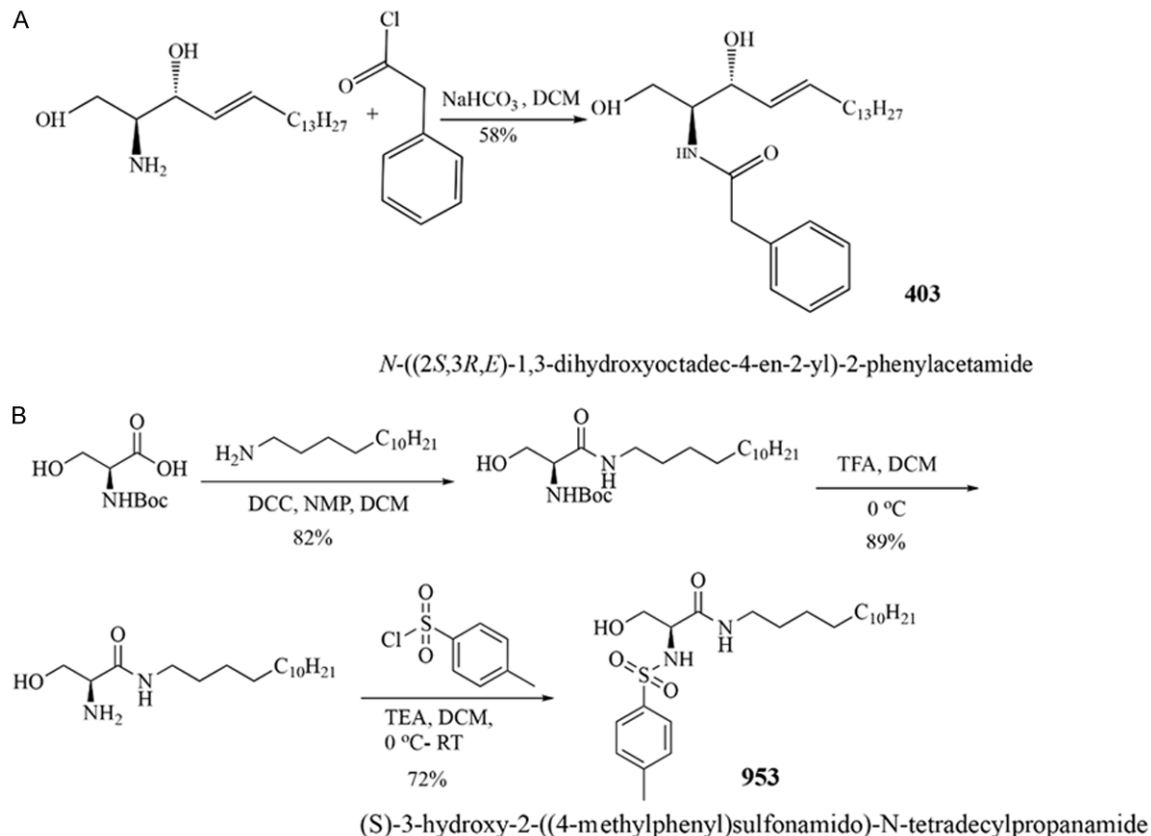
Figure 2. The synthesis schemes for ceramide analogs 403 and 953. A, B. The detailed synthesis procedures were described in the Methods.

vidual ceramide and dh-ceramide species between the A549 and H460 cell-lines. For example, both analogs 403 and 953 increased C14-Cer production in the A549 cells, but not in the H460 cells (**Figure 5A**, **5B**). For dh-ceramide species, analog 403 only increased dhC18-Cer and dhC20-Cer in the A549 cells, but not in the H460 cells. These data indicate putative heterogeneity for sphingolipid metabolism in NSCLC cells, which are potentially connected to cancer cell response to sphingolipid targeted therapies.

The composition and proportion of individual ceramide and dh-ceramide species can also be studied using lipidomics analyses. We previously showed the top predominant ceramide/dh-ceramide species identified within the NSCLC cell-lines, including C16-, C22-, C24:1-, C24-, dhC16-, dhC18-, dhC22-, dhC24:1- and dhC24-Cer [18]. Despite subtle differences, NSCLC cell-lines display a consistent ceramide signature. Here, we found that in the A549 cell-line, both analogs 403 and 953 increased the proportions of C16-, C22-, C24:1-, and dhC16-

Cer, while decreasing the proportions of C24- and dhC24-Cer. In comparison, ABC294640 increased the proportions of C22-, C24:1-, and dhC22-Cer, while decreasing the proportions of C16-, C24-, and dhC16-Cer. In the H460 cell-line, there are some variations between analog 403 and 953. They both increased the proportion of C22-Cer, while decreasing the proportions of C16- and dhC18-Cer. In addition, analog 403 increased the proportions of C24-, dhC16-, and dhC24-Cer, while decreasing the proportions of C24:1-, dhC22-, and dhC24:1-Cer. Analog 953 increased the proportion of dhC22-Cer, while decreasing the proportion of C24-Cer. In comparison, ABC294640 increased the proportions of dhC18- and dhC22-Cer, while decreasing the proportions of C16-, C24-, dhC16-, and dhC24:1-Cer (**Figure 7A**, **7B**).

Treatment with the two new ceramide analogs effectively represses NSCLC tumor growth in vivo

By using an established H460 xenograft mice model, the effects of analogs 403 and 953 on
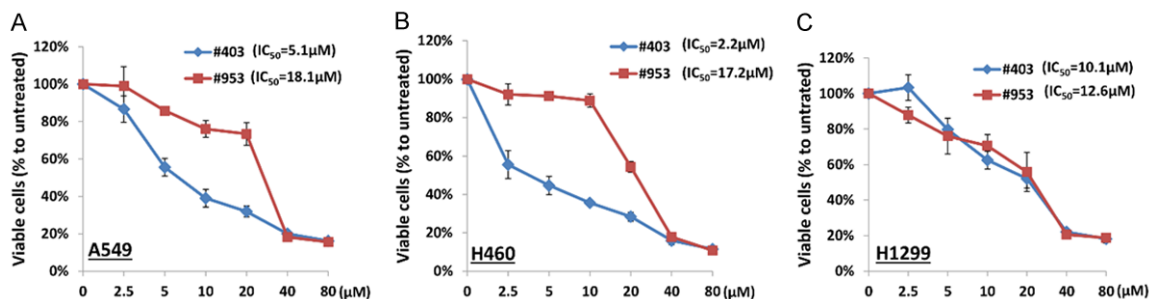
Figure 3. New ceramide analogs 403 and 953 treatments inhibit the growth of NSCLC cell-lines in a dose-dependent manner. A-C. NSCLC cell-lines A549, H460, and H1299 were incubated with the indicated concentrations of 403 or 953 for 72 h; cell proliferation was measured using the WST-1 assays. The 50% Inhibitory Concentrations (IC_{50}) were calculated by using GraphPad Prism 9. Error bars represent S.D. for 3 independent experiments.

NSCLC tumor growth were studied *in vivo*. H460 cells (5×10^5 cells, 1:1 with growth factor-depleted Matrigel) were injected subcutaneously into the flank of nude mice (5 mice per group). Five days after injection, the mice were randomly separated into three groups and received i.p. injections with vehicle, analog 403 or 953 (25 mg/kg of body weight, respectively), 3 days/week. The mice were observed every 2-3 days, and palpable tumors were measured over an additional 3 weeks. The results indicated that treatment with both analogs 403 and 953 significantly repressed tumor growth in mice when compared to those from the vehicle-treated mice (**Figure 8A**). Analog 403 showed slightly better efficacy than analog 953, although with no statistical significance between these two groups. Furthermore, we found both analogs 403 and 953 increased the expression of cleaved caspase 3 and 9, the markers of apoptosis from tumor tissues collected from analog-treated mice when compared to vehicle-treated mice (**Figure 8B**). No visible signs of toxicity, such as weight loss, were observed in the mice during the treatment period.

Discussion

All 7 newly synthesized ceramide analogs screened for activity in the three different NSCLC cell-lines studied effectively inhibited cancer cell growth, especially analogs 403 and 953. Interestingly, analogs 403 and 953 have significantly different chemical structures. Analog 403 has a 3-hydroxy-4-ene (enol) backbone structure similar to naturally occurring ceramides, with a modified side chain containing a phenylacetyl amide. Analog 953 has an

amide functionality in the backbone, and a sulfonamide functionality in the side chain containing a 4-methyl substituted phenyl group. On NSCLC cell-lines, the IC_{50}s of analogs 403 and 953 were at ~2-18 μM, which are comparable to those of SphK inhibitor, ABC294640 (~7-9 μM) in our previous study [18]. A recent study has reported a novel and small molecule SphK1/2 dual inhibitor, SKI-349, with IC_{50}s on primary NSCLC cells and immortalized cell-lines of ~5-10 μM [21]. In contrast, another recent study has reported the IC_{50} of exogenous C2-Cer on NSCLC cell-lines to be ~100 μM [22]. These data together highlight the potential of our ceramide analogs as promising candidates for sphingolipid-based NSCLC therapies.

Here we found that both analogs 403 and 953 caused significant apoptosis in NSCLC cell-lines, unrelated to cell cycle arrest (data not shown). These findings are not consistent with our previous study in which we found that some ceramide analogs caused obvious G1 and/or G2/M cell cycle arrest in virus-associated lymphoma cells [23]. This may be due to the varied response to ceramide analogs by different cancer types. Sphingolipid metabolism regulates various cellular factors that influence cell survival and death. Our previous microarray analysis identified specific cellular genes affected by ceramide analogs, such as *AURKA* (Aurora A kinase) and *CDCA3* (cell division cycle-associated 3), which play crucial roles in the survival of virus-associated lymphoma cells [23]. Additionally, exogenous ceramide-induced apoptosis in NSCLC cells has been linked to the Txnip/Trx1 complex [22]. The thioredoxin-interacting protein (Txnip) regulates a
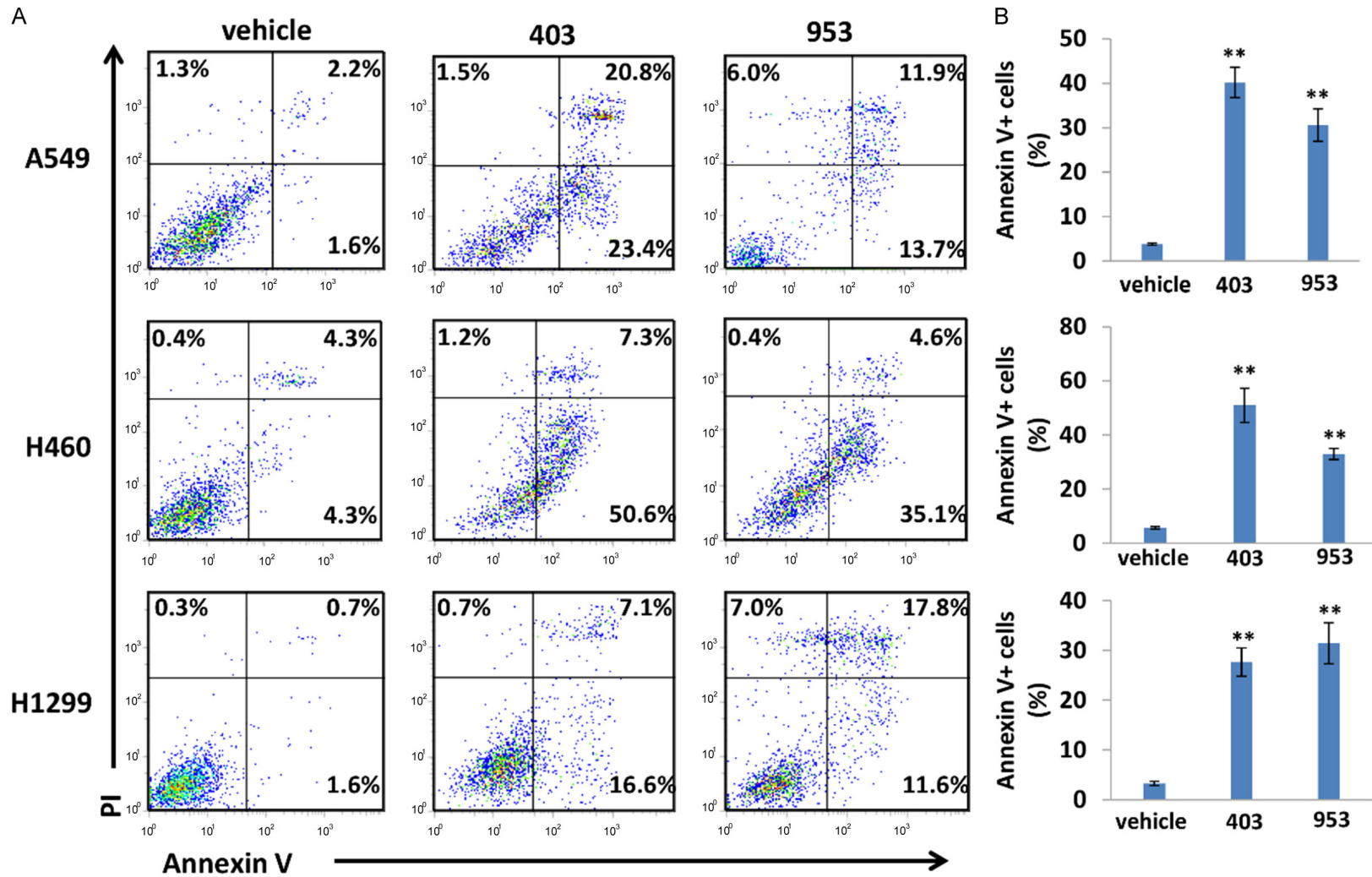
Figure 4. Treatment with the new ceramides 403 and 953 induce significant apoptosis in NSCLC cell-lines. A, B. NSCLC cell-lines A549, H460, and H1299 were incubated with 20 μM of ceramide analog 403, 953 or vehicle for 48 h; cell apoptosis was measured using Annexin V-PI staining and flow cytometry analysis. Error bars represent the S.D. from 3 independent experiments. ** = P<0.01.

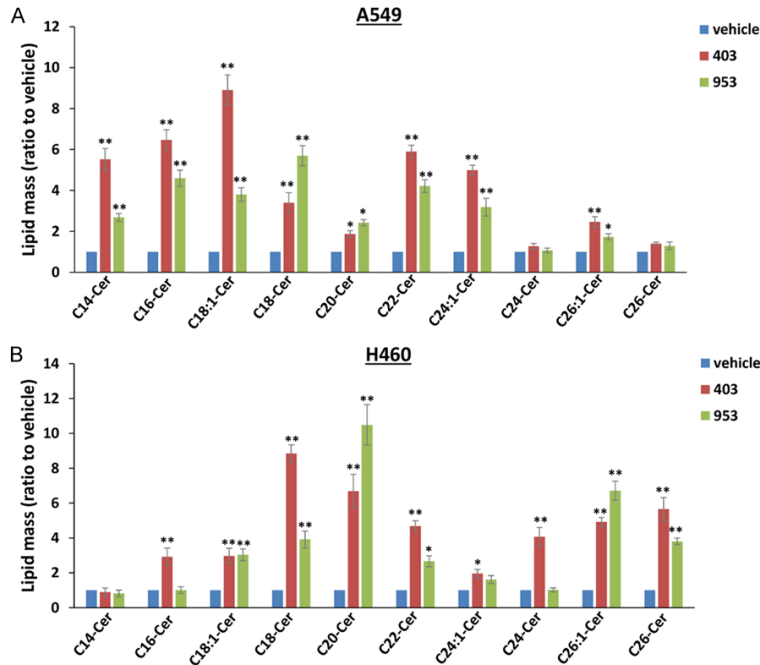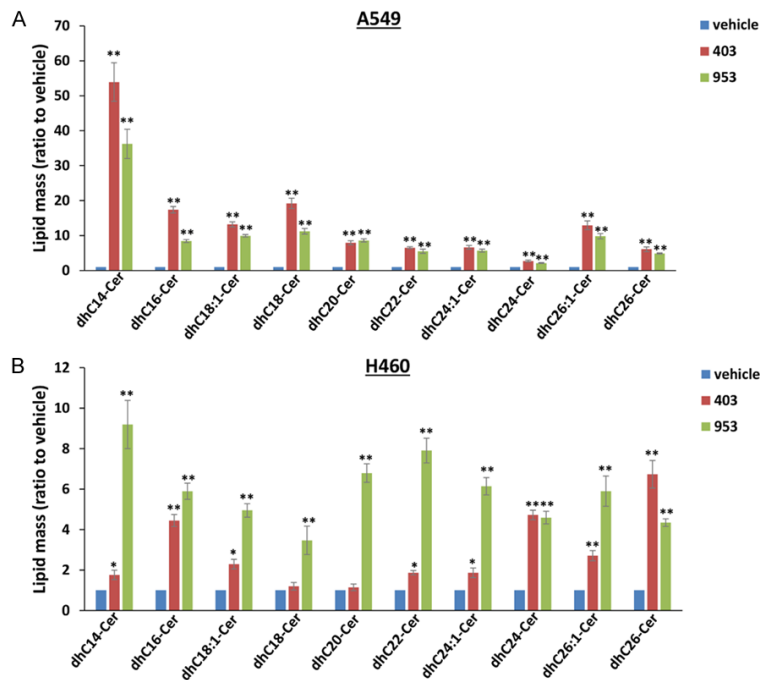**Figure 5.** New ceramide analogs 403 and 953 treatments induce intracellular ceramides production from NSCLC cell-lines. (A, B) NSCLC cell-lines A549 (A) and H460 (B) were incubated with 20 µM of ceramide analog 403, 953 or vehicle for 48 h; ceramide species were quantified using lipidomics analysis as described in the Methods. Error bars represent the S.D. from 3 independent experiments. * = P<0.05, ** = P<0.01.

Figure 6. New ceramide analogs 403 and 953 treatments induce intracellular dh-ceramides production from NSCLC cell-lines. (A, B) NSCLC cell-lines A549 (A) and H460 (B) were incubated with 20 µM of ceramide analog 403, 953 or vehicle for 48 h; dihydro(dh)-ceramide species were quantified using lipidomics analysis as described in the Methods. Error bars represent the S.D. from 3 independent experiments. * = P<0.05, ** = P<0.01.

variety of oxidative stresses together with glutathione; it can also inhibit the exchange between the disulfide bonds of thioredoxin (Trx)1 to inhibit the reducing activity of Trx [24-27]. As we know, Trx is an important redox regulator and a sensor of energy and glucose metabolism, involved in various physiological processes including cell apoptosis. Thus, understanding the intricate mechanisms underlying the apoptosis induced by these new ceramide analogs in NSCLC cells requires further investigation.

Our lipidomics analyses revealed changes in the proportions of major ceramide and dh-ceramide species induced by the two ceramide analogs in NSCLC cell-lines. Three key findings emerged from these analyses: 1) Variations in the changes of proportion between NSCLC cell-lines highlight tumor heterogeneity and the diverse responses to the same treatment; 2) Distinct changes in proportion by analogs 403 and 953 underscore the varied impacts of different chemical structures of ceramide analogs on sphingolipid metabolism in NSCLC; and 3) Discrepancies in the changes of proportion between ceramide analogs and the SphK inhibitor suggest that ceramide analogs may influence not only SphK but also other components of sphingolipid metabolism in NSCLC. Our previous work demonstrated that certain ceramide analogs, including analog 403, reduced the expression of ceramide metabolizing enzymes such as SphK1, SphK2, and glucosylceramide synthase (GCS) in virus-associated lymphomas [23]. Future investigations will focus on
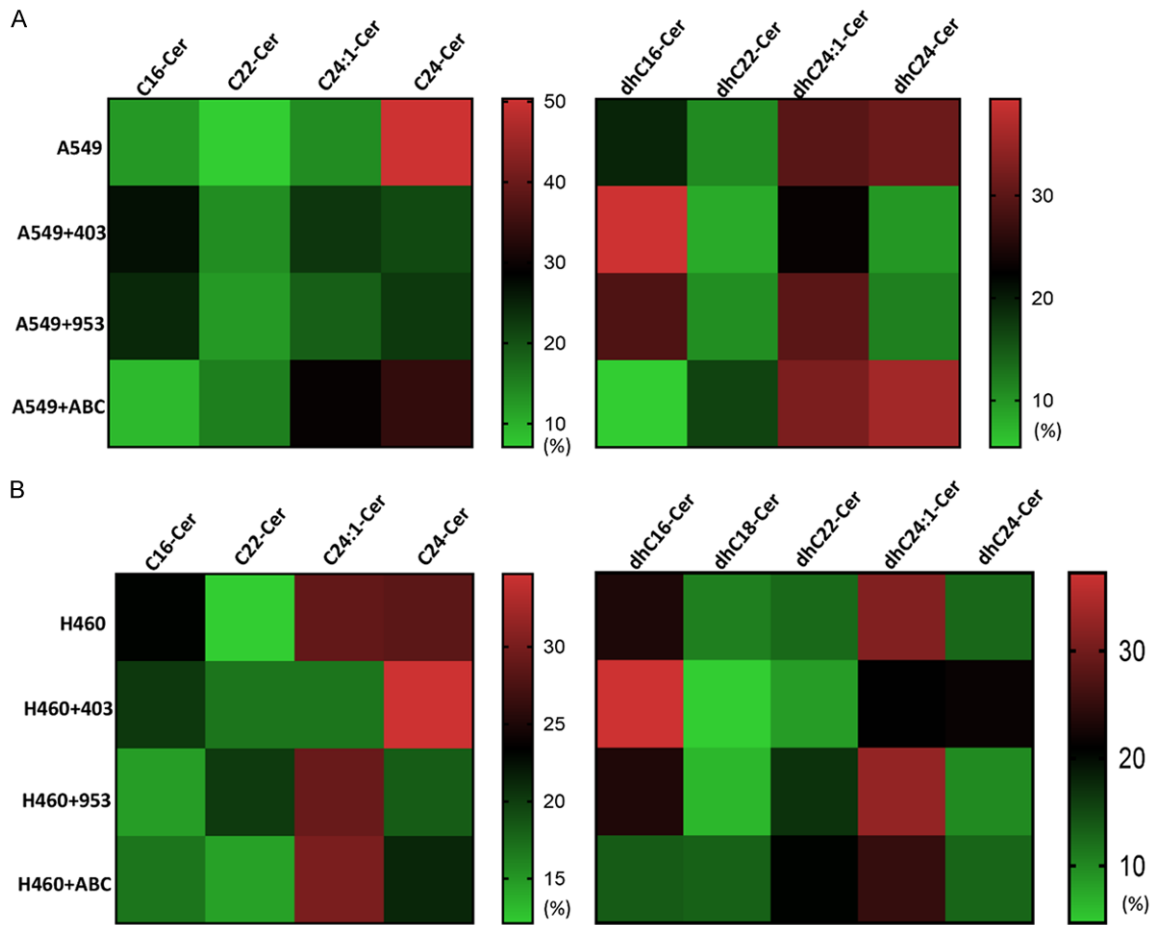
Figure 7. The proportions of major ceramide/dh-ceramide species in NSCLC cell-lines are altered by new ceramide analogs. (A, B) Heatmaps showed relative proportions of major ceramide and dh-ceramide species upregulated or downregulated by analog 403 or 953 in NSCLC cell-lines, A549 (A) and H460 (B), respectively. The SphK2 inhibitor, ABC294640 (ABC), was used as a comparison.
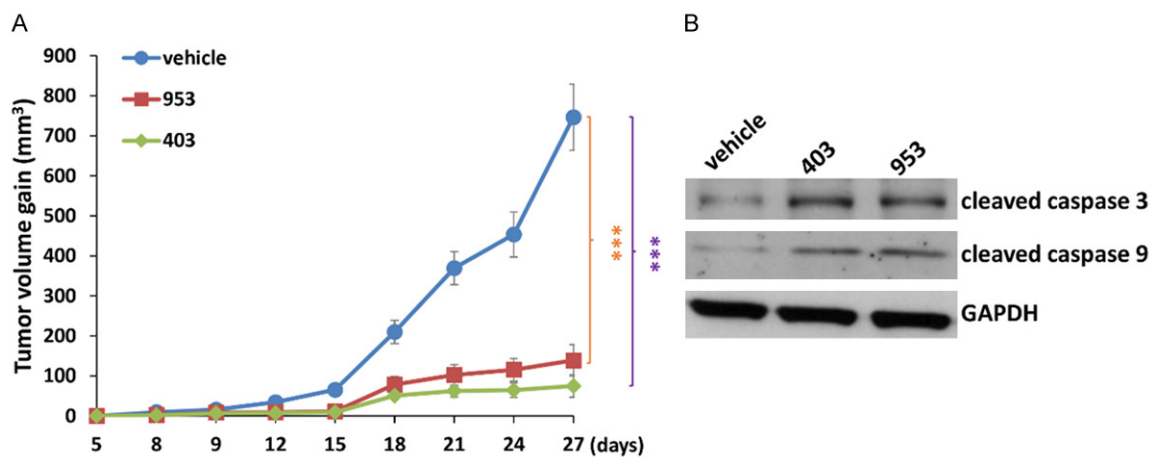

Figure 8. Treatment with the new ceramide analogs suppresses NSCLC growth *in vivo*. A. NSCLC H460 cells (5×10^5 cells, 1:1 with growth factor-depleted Matrigel) were injected subcutaneously into the flank of nude mice. Five days after this injection, the mice were randomly separated into three groups and received i.p. injection with either vehicle, ceramide analog 403 or 953 (25 mg/kg of body weight, respectively), 3 days/week. The mice were observed and measured every 2-3 days for the size of palpable tumors over an additional 3 weeks. Error bars represent the S.D. of tumor volume gain from the same group mice (n = 5 per group). *** = P<0.001. B. Protein expression within tumor tissues from representative treated mice was measured by using immunoblots.

elucidating how these ceramide analogs regulate various ceramide-synthesizing or metabolizing enzymes and understanding the connections between changes in the proportions of major ceramide and dh-ceramide species and NSCLC cell survival and growth.

Acknowledgements

Disclosure of conflict of interest

None.

Address correspondence to: Dr. Zhiqiang Qin, Department of Pathology, Winthrop P. Rockefeller Cancer Institute, University of Arkansas for Medical Sciences, 4301 W. Markham St., Little Rock, AR 72205, USA. Tel: 501-526-8619; E-mail: zqin@uams.edu; Dr. Maryam Foroozesh, Department of Chemistry, Xavier University of Louisiana, 1 Drexel Drive, New Orleans, LA 70125, USA. Tel: 504-520-5078; E-mail: mforooze@xula.edu

References

[1] American Cancer Society. Cancer Facts & Figures 2017. Atlanta: American Cancer Society; 2017.

[2] Jemal A, Siegel R, Ward E, Hao Y, Xu J and Thun MJ. Cancer statistics, 2009. CA Cancer J Clin 2009; 59: 225-249.

[3] Molina JR, Yang P, Cassivi SD, Schild SE and Adjei AA. Non-small cell lung cancer: epidemiology, risk factors, treatment, and survivorship. Mayo Clin Proc 2008; 83: 584-594.

[4] Ware KE, Hinz TK, Kleczko E, Singleton KR, Marek LA, Helfrich BA, Cummings CT, Graham DK, Astling D, Tan AC and Heasley LE. A mechanism of resistance to gefitinib mediated by cellular reprogramming and the acquisition of an FGF2-FGFR1 autocrine growth loop. Oncogenesis 2013; 2: e39.

[5] Sundar R, Cho BC, Brahmer JR and Soo RA. Nivolumab in NSCLC: latest evidence and clinical potential. Ther Adv Med Oncol 2015; 7: 85-96.

[6] Andrews A. Treating with checkpoint inhibitors-figure $1 million per patient. Am Health Drug Benefits 2015; 8: 9.

[7] Gainor JF, Shaw AT, Sequist LV, Fu X, Azzoli CG, Piotrowska Z, Huynh TG, Zhao L, Fulton L, Schultz KR, Howe E, Farago AF, Sullivan RJ, Stone JR, Digumarthy S, Moran T, Hata AN, Yagi Y, Yeap BY, Engelman JA and Mino-Kenudson M. EGFR mutations and ALK rearrangements are associated with low response rates to PD-1 pathway blockade in non-small cell lung cancer: a retrospective analysis. Clin Cancer Res 2016; 22: 4585-4593.

[8] Lo Russo G, Moro M, Sommariva M, Cancila V, Boeri M, Centonze G, Ferro S, Ganzinelli M, Gasparini P, Huber V, Milione M, Porcu L, Proto C, Pruneri G, Signorelli D, Sangaletti S, Sfondrini L, Storti C, Tassi E, Bardelli A, Marsoni S, Torri V, Tripodo C, Colombo MP, Anichini A, Rivoltini L, Balsari A, Sozzi G and Garassino MC. Antibody-Fc/FcR interaction on macrophages as a mechanism for hyperprogressive disease in non-small cell lung cancer subsequent to PD-1/PD-L1 blockade. Clin Cancer Res 2019; 25: 989-999.

[9] Ogretmen B. Sphingolipid metabolism in cancer signalling and therapy. Nat Rev Cancer 2018; 18: 33-50.

[10] Cuvillier O, Pirianov G, Kleuser B, Vanek PG, Coso OA, Gutkind S and Spiegel S. Suppression of ceramide-mediated programmed cell death by sphingosine-1-phosphate. Nature 1996; 381: 800-803.

[11] French KJ, Schrecengost RS, Lee BD, Zhuang Y, Smith SN, Eberly JL, Yun JK and Smith CD. Discovery and evaluation of inhibitors of human sphingosine kinase. Cancer Res 2003; 63: 5962-5969.

[12] French KJ, Zhuang Y, Maines LW, Gao P, Wang W, Beljanski V, Upson JJ, Green CL, Keller SN and Smith CD. Pharmacology and antitumor activity of ABC294640, a selective inhibitor of sphingosine kinase-2. J Pharmacol Exp Ther 2010; 333: 129-139.

[13] Qin Z, Dai L, Trillo-Tinoco J, Senkal C, Wang W, Reske T, Bonstaff K, Del Valle L, Rodriguez P,

Flemington E, Voelkel-Johnson C, Smith CD, Ogretmen B and Parsons C. Targeting sphingosine kinase induces apoptosis and tumor regression for KSHV-associated primary effusion lymphoma. Mol Cancer Ther 2014; 13: 154-164.

[14] Venant H, Rahmaniyan M, Jones EE, Lu P, Lilly MB, Garrett-Mayer E, Drake RR, Kraveka JM, Smith CD and Voelkel-Johnson C. The sphingosine kinase 2 inhibitor ABC294640 reduces the growth of prostate cancer cells and results in accumulation of dihydroceramides in vitro and in vivo. Mol Cancer Ther 2015; 14: 2744-2752.

[15] Xun C, Chen MB, Qi L, Tie-Ning Z, Peng X, Ning L, Zhi-Xiao C and Li-Wei W. Targeting sphingosine kinase 2 (SphK2) by ABC294640 inhibits colorectal cancer cell growth in vitro and in vivo. J Exp Clin Cancer Res 2015; 34: 94.

[16] Lewis CS, Voelkel-Johnson C and Smith CD. Suppression of c-Myc and RRM2 expression in pancreatic cancer cells by the sphingosine kinase-2 inhibitor ABC294640. Oncotarget 2016; 7: 60181-60192.

[17] Britten CD, Garrett-Mayer E, Chin SH, Shirai K, Ogretmen B, Bentz TA, Brisendine A, Anderton K, Cusack SL, Maines LW, Zhuang Y, Smith CD and Thomas MB. A phase I study of ABC294640, a first-in-class sphingosine kinase-2 inhibitor, in patients with advanced solid tumors. Clin Cancer Res 2017; 23: 4642-4650.

[18] Dai L, Smith CD, Foroozesh M, Miele L and Qin Z. The sphingosine kinase 2 inhibitor ABC294640 displays anti-non-small cell lung cancer activities in vitro and in vivo. Int J Cancer 2018; 142: 2153-2162.

[19] Ponnapakam AP, Liu J, Bhinge KN, Drew BA, Wang TL, Antoon JW, Nguyen TT, Dupart PS, Wang Y, Zhao M, Liu YY, Foroozesh M and Beckman BS. 3-Ketone-4,6-diene ceramide analogs exclusively induce apoptosis in chemo-resistant cancer cells. Bioorg Med Chem 2014; 22: 1412-1420.

[20] Bielawski J, Szulc ZM, Hannun YA and Bielawska A. Simultaneous quantitative analysis of bioactive sphingolipids by high-performance liquid chromatography-tandem mass spectrometry. Methods 2006; 39: 82-91.

[21] Xue Y, Jiang K, Ou L, Shen M, Yang Y, Lu J and Xu W. Targeting sphingosine kinase 1/2 by a novel dual inhibitor SKI-349 suppresses non-small cell lung cancer cell growth. Cell Death Dis 2022; 13: 602.

[22] Shi Y, Jin Y, Liu F, Jiang J, Cao J, Lu Y and Yang J. Ceramide induces the apoptosis of non-small cell lung cancer cells through the Txnip/Trx1 complex. Int J Mol Med 2021; 47: 85.

[23] Chen J, Goyal N, Dai L, Lin Z, Del Valle L, Zabaleta J, Liu J, Post SR, Foroozesh M and Qin Z. Developing new ceramide analogs and identifying novel sphingolipid-controlled genes against a virus-associated lymphoma. Blood 2020; 136: 2175-2187.

[24] Xu L, Lin X, Guan M, Zeng Y and Liu Y. Verapamil attenuated prediabetic neuropathy in high-fat diet-fed mice through inhibiting TXNIP-mediated apoptosis and inflammation. Oxid Med Cell Longev 2019; 2019: 1896041.

[25] Kizhakkayil J, Thayyullathil F, Chathoth S, Hago A, Patel M and Galadari S. Glutathione regulates caspase-dependent ceramide production and curcumin-induced apoptosis in human leukemic cells. Free Radic Biol Med 2012; 52: 1854-1864.

[26] Xu W, Wang L, Li J, Cai Y and Xue Y. TXNIP mediated the oxidative stress response in glomerular mesangial cells partially through AMPK pathway. Biomed Pharmacother 2018; 107: 785-792.

[27] Lv H, Zhu C, Wei W, Lv X, Yu Q, Deng X and Ci X. Enhanced Keap1-Nrf2/Trx-1 axis by daphnetin protects against oxidative stress-driven hepatotoxicity via inhibiting ASK1/JNK and Txnip/NLRP3 inflammasome activation. Phytomedicine 2020; 71: 153241.